

The ρ Spectral Function in a Relativistic Resonance Model *

M. Post, S. Leupold and U. Mosel

*Institut für Theoretische Physik, Universität Giessen,
D-35392 Giessen, Germany*

Abstract

We calculate the spectral function A_ρ of the ρ meson in nuclear matter. The calculation is performed in the *low density* approximation, where the in-medium self energy Σ_{med} is completely determined by the vacuum ρN forward scattering amplitude. This amplitude is derived from a relativistic resonance model. In comparison to previous non-relativistic calculations we find a much weaker momentum dependence of Σ_{med} , especially in the transverse channel. Special attention is paid to uncertainties in the model. Thus, we compare the impact of different coupling schemes for the $RN\rho$ interaction on the results and discuss various resonance parameter sets.

PACS: 21.65.+f, 12.38.Lg, 14.40.Cs, 13.60.Lg

Keywords: Rho Spectral Function, Nuclear Matter, Nucleon Resonance, Breit-Wigner Model

*Work supported by BMBF and DFG.

1 Introduction

The question of how vector meson properties change at finite baryon density or temperature has triggered a lot of theoretical and experimental work in the last decade. Of particular interest are the in-medium properties of ρ and a_1 meson, which are chiral partners. One of the most evident signatures of the spontaneous breaking of chiral symmetry in vacuum is the large mass difference between these mesons. The claim is that the in-medium mass spectra of ρ and a_1 meson can be related to the partial restoration of chiral symmetry. If a chirally symmetric phase is reached at high density/temperature, a degeneracy of their spectral functions is expected [1, 2]. Whereas only a few studies exist on the in-medium properties of the a_1 meson [3, 4], numerous theoretical works have been performed for the ρ meson [5, 6, 7, 8, 9, 10, 11, 12, 13, 14, 15, 16].

It has been argued by several groups that the mass of the ρ meson is related to the expectation value of the scalar quark condensate. The latter is supposed to decrease at finite nuclear density due to the restoration of chiral symmetry, thereby inducing a mass shift on the ρ meson. The most famous of these models is that of Brown and Rho [5]. It predicts a downward shift for the ρ meson mass of about 15% – 20% at normal nuclear matter density. Similar results have been found in [6] using the QCD sum rule approach under the assumption that the width of the ρ meson remains small in the nuclear medium (cf. [7] for a thorough discussion of that point).

In other approaches the properties of the ρ meson in nuclear matter are calculated by taking into account conventional nuclear many body effects. At low densities the self energy Σ_{med} can be calculated in the ρT approximation and is completely determined by the knowledge of the vacuum ρN forward scattering amplitude T . Since this quantity is not directly accessible by experiment, one needs to construct a model which incorporates experimental constraints as far as possible. This was first pointed out in [8]. Information on ρN scattering comes mostly from $\pi N \rightarrow \pi \pi N$ processes. One of the most successful descriptions of these reactions has been achieved by Manley *et al* within an isobar model [17, 18].

A resonance model for the ρN scattering amplitude allows the incorporation of experimental constraints in a straightforward fashion. Such a strategy was first suggested in [9], where only p -wave resonances were taken into account. However, as shown in our previous paper [10], the $D_{13}(1520)$

resonance plays a dominant role in ρN scattering and can therefore not be neglected in a complete analysis. In both models the resonance parameters were taken from the PDG [19] and the calculation was performed within a non-relativistic framework. An alternative approach has been chosen in [8, 11], where the baryonic resonances are not introduced as excited three-quark states, but are generated dynamically in a coupled channel approach from meson-nucleon and meson- Δ rescattering. In [12] the ρN scattering amplitude is derived from an effective chiral Lagrangian theory, neglecting, however, resonant contributions.

Going beyond the low density approximation, various groups have considered the change in the 2π decay of the ρ as induced by the modified π spectrum in the nuclear medium, see e.g. [13, 14, 15, 16]. In [15, 16] resonance contributions have also been included.

Qualitatively, all these models predict a strong broadening of the ρ meson. The mass, however, remains nearly unchanged. This finding is in good agreement with QCD sum rules, see e.g. [7, 12].

So far experimental signals indicating a change of the ρ spectrum in the nuclear medium, have been obtained by the CERES [20, 21] and the HELIOS collaboration [22]. In these experiments the dilepton spectra display a downward-shift of strength in the region of the ρ meson as compared to theoretical predictions. Agreement between theory and experiment can be reached by introducing medium modifications for the ρ meson [23]. On the other hand, in [24] the claim is made, that the CERES data do not necessarily hint to a medium modification of the ρ meson, but can also be explained with its vacuum properties.

Certainly, in order to gain a more quantitative understanding of the ρ meson properties in nuclear matter, further theoretical studies, especially on the momentum dependence of the spectral function, and improved experimental statistics, are mandatory. The sensitivity on details of the spectral function is even enhanced in photo-nuclear reactions, as was demonstrated in [25].

The aim of this paper is to examine up to which extent safe conclusions about the propagation of ρ mesons in nuclear matter can be drawn from a resonance model. We therefore do not only lift the non-relativistic approximation, but also study the dependence of the results on various coupling schemes. Furthermore, we analyse the influence of different resonance parameter sets on the results.

The paper is organized as follows. In Sect. 2 we will present an overview of the formalism employed to describe the spectral function. Furthermore, an arbitrariness in the non-relativistic approach is exposed and thus the need for a relativistic model is motivated. The basic ingredients of the relativistic calculation will be introduced in Sect. 3. A problem related with the description of the resonance propagator and its solution is presented in Sect. 3.1. In Sect. 4 we analyze the quality and properties of different resonance parameter sets and their influence on the results. In Sect. 5 the results of the relativistic calculation are presented and then compared to the non-relativistic calculation. The impact of various coupling schemes for the vertex $RN\rho$ is studied in Sect. 6. We summarize our results in Sect. 7.

2 Overview of the Model

In this section we explain the formalism on which our calculation of the in-medium spectral function of the ρ meson is based and introduce some basic notation. We then review our previous non-relativistic results [10] and use some simple kinematical considerations to point out why a fully relativistic framework is needed.

2.1 Definition of the Basic Quantities

The spectral function is defined as the imaginary part of the propagator. Due to Lorentz invariance the vacuum spectral function of the ρ meson depends only on one kinematic variable – its invariant mass – and both transverse and longitudinal modes have the same spectral distribution. The presence of nuclear matter breaks Lorentz invariance. Consequently transverse and longitudinal propagation modes of the ρ meson receive different in-medium modification. Also, the corresponding spectral functions depend both on the energy ω of the ρ meson and its three-momentum \mathbf{q} :

$$A_\rho^{T/L}(\omega, \mathbf{q}) = \frac{1}{\pi} \frac{\text{Im } \Sigma^{T/L}(\omega, \mathbf{q})}{(\omega^2 - \mathbf{q}^2 - m_\rho^2 + \text{Re } \Sigma^{T/L}(\omega, \mathbf{q}))^2 + \text{Im } \Sigma^{T/L}(\omega, \mathbf{q})^2} \quad . \quad (1)$$

m_ρ is the pole mass of the ρ meson. $\Sigma^{T/L}$ is the transverse or longitudinal part of the self energy of the ρ meson and can be decomposed into a vacuum

and an in-medium part:

$$\Sigma^{T/L}(\omega, \mathbf{q}) = \Sigma_{vac}(m) + \Sigma_{med}^{T/L}(\omega, \mathbf{q}) \quad . \quad (2)$$

The imaginary part of the former is to lowest order in the coupling constant given by the 2-pion decay width of the ρ meson [12, 14]:

$$\text{Im } \Sigma_{vac}(m) = m \Gamma_{\pi\pi}(m) \quad , \quad (3)$$

and

$$\Gamma_{\pi\pi}(m) = \left(\frac{m_\rho}{m}\right)^2 \Gamma_0 \left(\frac{\mathbf{p}_m}{\mathbf{p}_{m_\rho}}\right)^3 \quad . \quad (4)$$

Here m is the invariant mass of the ρ meson, Γ_0 its decay width on the pole mass and \mathbf{p}_{m_ρ} (\mathbf{p}_m) denotes the 3-momentum of the pions measured in the rest frame of a decaying ρ meson with mass m_ρ (m). For invariant masses of the ρ meson up to around 1 GeV - which we consider in this paper - the real part of $\Sigma_{vac}(m)$ shows only small variations and can be neglected.

At finite nucleon density ρ_N the in-medium self energy Σ_{med} is obtained in the $\rho_N T$ approximation [26]:

$$\Sigma_{med}^{T/L}(q, p_N) = \frac{1}{8m_N} \rho_N T_{tot}^{T/L}(q, p_N) \quad . \quad (5)$$

In our notation q and p_N are the 4-vectors of ρ meson and nucleon, respectively. T_{tot} is the ρN forward scattering amplitude. It is obtained as a sum over all included resonances. For a single resonance the scattering amplitude is depicted in Fig. 1. The corresponding contribution to the transverse and longitudinal channel is obtained from the tensor $T^{\mu\nu}(q, p_N)$ upon contracting with the projection operators $P_{\mu\nu}^{T/L}$ [10, 12, 15]:

$$\begin{aligned} T^T &= \frac{1}{2} T^{\mu\nu} P_{\mu\nu}^T \\ T^L &= T^{\mu\nu} P_{\mu\nu}^L \quad . \end{aligned} \quad (6)$$

The general form of $T^{\mu\nu}(q, p_N)$ reads:

$$T^{\mu\nu}(q, p_N) = \begin{cases} f^2 \text{Tr } \mathcal{V}_{\frac{1}{2}}^\mu(q, p_N) D_{\frac{1}{2}}(k) \mathcal{V}_{\frac{1}{2}}^\nu(q, p_N) (\not{p} + m_N) & \text{for } J = \frac{1}{2}, \\ f^2 \text{Tr } \mathcal{V}_{\frac{3}{2}}^{\mu\alpha}(q, p_N) D_{\frac{3}{2} \alpha\beta}(k) \mathcal{V}_{\frac{3}{2}}^{\beta\nu}(q, p_N) (\not{p} + m_N) & \text{for } J = \frac{3}{2}, \end{cases} \quad (7)$$

where $k = p_N + q$ is the four-momentum of the intermediate resonance. The coupling strength at the $RN\rho$ vertex is given by f . A detailed discussion of both the relativistic vertex functions $\mathcal{V}_{\frac{1}{2}}^\mu(q, p_N)$ and $\mathcal{V}_{\frac{3}{2}}^{\mu\nu}(q, p_N)$ as well as the relativistic propagators of spin- $\frac{1}{2}$ and spin- $\frac{3}{2}$ resonances $D_{\frac{1}{2}}(k)$ and $D_{\frac{3}{2}}^{\alpha\beta}(k)$ will follow in Sect. 3 and 3.1.

The coupling constant f is obtained from a fit to the measured partial decay width $R \rightarrow N\rho$. In Sect. 4 we discuss thoroughly from which analysis the resonance parameters are taken. Since many of the resonances which are considered in this work are below or relatively close to the nominal threshold for this decay of $\sqrt{s} = m_N + m_\rho \approx 1.7$ GeV, we integrate over the vacuum spectral function of the ρ meson (see Fig. 2). The decay width then reads:

$$\Gamma_{N\rho}(s) = \frac{1}{2j_R + 1} \frac{I_\Gamma}{8\pi s} \int_{2m_\pi}^{\sqrt{s}-m_N} dm 2m F(s)^2 \times A_\rho^{vac}(m^2) (2|\mathcal{M}_{RN\rho}^T|^2 + |\mathcal{M}_{RN\rho}^L|^2) q_{cm} \quad . \quad (8)$$

The spin of the resonance is denoted by j_R , I_Γ is an isospin factor. A_ρ^{vac} is the vacuum spectral function of the ρ meson. By q_{cm} we denote the momentum of the ρ meson in the rest frame of the decaying resonance. The squared matrix element for the resonance decay $|\mathcal{M}_{RN\rho}^{T(L)}|^2$ reads in terms of the vertex functions \mathcal{V} (here for spin- $\frac{1}{2}$ resonances):

$$|\mathcal{M}_{RN\rho}^{T(L)}|^2 = -f^2 \frac{P_{\mu\nu}^T}{2} (P_{\mu\nu}^L) \sum_{s,r} \bar{u}_r^R(k) \mathcal{V}_{\frac{1}{2}}^\mu u_s(p_N) \bar{u}_s(p_N) \mathcal{V}_{\frac{1}{2}}^\nu u_r^R(k) \quad . \quad (9)$$

The spinors $u_r^R(k)$ and $u_s(p_N)$ denote resonance and nucleon spinors respectively. The numerical values for f , which we obtain this way, are given in Table 1. The formfactor $F(s)$ will be explained in Eq. 18. We have defined $\Gamma_{N\rho}$ for an arbitrary invariant mass \sqrt{s} of the resonance, since we use Eq. 8 also as a parameterization of the mass dependence of the decay width.

The low-density ρT approximation Eq. 5 only describes two-body processes in the nuclear medium. At sufficiently large densities also higher order effects need to be taken into account – currently, however, a scale that pins down the breakdown of the ρT approximation is not at hand. A comprehensive description of many-body effects is very hard to obtain [10, 16] and beyond the scope of this work. Therefore, we incorporate only two typical in-medium corrections to the low-density approximation:

- integration over the Fermi sphere of the nucleons,
- renormalization of Σ_{med} due to short range correlations.

In the case of p -wave resonances, the short range correlations are incorporated via the Landau-Migdal parameters:

$$\Sigma_{med}(\omega, \mathbf{q}) = \frac{\Sigma_{med}}{1 - g' \frac{\Sigma_{med}}{\mathbf{q}^2}} \quad . \quad (10)$$

Only the $P_{33}(1232)$ is renormalized, leading to a suppression of its contribution. For the Landau-Migdal parameter we take $g' = 0.5$. For higher p -wave resonances this parameter is not known. The actual calculation shows very little effect on the results. For s -wave resonances there is no information available as how to include short range correlations. Thus, we do not include it for those resonances.

2.2 Critical Review of the Non-Relativistic Model

Up to now all calculations of the in-medium properties of the ρ meson within a resonance model have considered a non-relativistic reduction of Eq. 7 [9, 10, 15, 16]. Let us therefore quickly review the qualitative features of the results of this approach as found in our previous work [10]. At low momenta the results are completely determined by the properties of the excited resonances. Their quantum numbers and experimentally observed coupling strengths to the ρN channel provide the necessary information. Close to threshold the resonance contribution scales like \mathbf{q}^{2l} , where \mathbf{q} is the momentum of the ρ meson. Consequently, at small values of \mathbf{q} s -wave resonances ($P = -1$) yield finite contributions, whereas the contribution from p -wave resonances ($P = +1$) is negligible. Quantitatively, the results of our explicit calculation of Σ_{med} [10] reveal that the propagation of a ρ meson in nuclear matter is dominated by the s -wave resonances $D_{13}(1520)$ and $D_{33}(1700)$ as a direct consequence of their large coupling to the ρN channel as given in [19]. The spectral function receives a rich structure: a new peak arises at an invariant mass of about 0.5 GeV from the excitation of the $D_{13}(1520)$ and the peak at the pole mass of the ρ meson is broadened by the $D_{33}(1700)$.

Whereas at low momenta the main uncertainty of the results comes from the values of the coupling constants, at high momenta an additional model

dependence is introduced by the momentum dependence of the self energy. In a non-relativistic calculation p -wave resonances do not couple to longitudinal ρ mesons. Furthermore, A^T and A^L display a completely different behaviour at high momenta. For A^L the effects from resonance excitation are rather small and the spectral function is strongly peaked at the ρ mass. A^T , in contrast, is completely smeared out in this kinematic regime.

We will demonstrate now that the momentum dependence of the self energy can not be reliably determined within a non-relativistic calculation and we argue that therefore a relativistic framework is imperative in order to put the results on a more solid basis.

The forward scattering amplitude is proportional to $f^2 \mathcal{V}^2$, see Eq. 7. From Eqs. 8 and 9 it is clear that the vertex function \mathcal{V} enters also into the determination of the coupling constant f . It thus appears twice in the forward scattering amplitude. An ambiguity now arises in the choice of the reference frame in which the non-relativistic matrix element is evaluated. In all previous works [9, 10, 15, 16] the following choice was made: the coupling constant was obtained by evaluating the matrix element in the CM frame (rest frame of the resonance) whereas the self energy was calculated in the LAB frame (rest frame of nuclear matter). This is a suggestive choice since the decay width is usually defined in the rest frame of the decaying particle whereas a nuclear matter calculation is preferably performed in the rest frame of nuclear matter. The non-relativistic reduction itself does not uniquely determine the reference frame, as it assumes that both the resonance and nucleon momentum are small compared to their masses. This condition is equally well met in the CM frame and in the LAB frame.

As shown in [9, 10], for a resonance of positive parity both the resonance decay width and the forward scattering amplitude are proportional to \mathbf{q}^2 . For a given invariant energy \sqrt{s} the three-momenta in LAB frame and CM frame are easily related:

$$q_{lab} = q_{cm} \frac{\sqrt{s}}{m_N} \quad . \quad (11)$$

The coupling constant f is adjusted to the decay width (see Eq. 8 and discussion). Computing the vertex function either in the CM frame or in the LAB frame leads to the following relation between the resulting coupling

constants:

$$f_{lab}^2 = f_{cm}^2 \frac{m_N^2}{m_R^2} \quad . \quad (12)$$

The most relevant contribution from each resonance to the self energy comes from the kinematical region $\sqrt{s} \approx m_R$ where the forward scattering amplitude obeys

$$T_{lab}^2 = T_{cm}^2 \frac{m_R^2}{m_N^2} \quad . \quad (13)$$

It is evident that the consistent use of either LAB frame or CM frame kinematics for both the determination of the coupling constant and the forward scattering amplitude leads to the same results. In contrast, the previously applied method of mixed kinematics [9, 10, 15, 16] produces an in-medium self energy which is larger by a factor of $\left(\frac{m_R}{m_N}\right)^2$. Typically, the resonance masses vary between 1.5 and 2 GeV. Thus for p -wave resonances the ambiguity in the non-relativistic reduction leads to uncertainties which can be as large as a factor of four. For s -wave resonances the effects are less pronounced. Here the transverse and the longitudinal channel are proportional to the energy ω^2 and the invariant mass q^2 of the ρ meson respectively. Thus only the transverse channel will be affected by the ambiguity of the reference frame. Noticeable uncertainties for Σ_{med} are expected for momenta comparable to the invariant mass of the ρ . Altogether, this is clearly not a satisfying situation which can only be resolved within a relativistic approach.

3 Relativistic Framework

In this Section we set up the relativistic framework for the calculation of Σ_{med} . We will present the Lagrangians used to describe the $RN\rho$ interaction. A discussion of the resonance propagator will be deferred to Sect. 3.1.

The vertex functions $\mathcal{V}_{\frac{1}{2}}^\mu$ and $\mathcal{V}_{\frac{3}{2}}^{\mu\nu}$ are derived from the following relativistic

and gauge invariant Lagrangians:

$$\mathcal{L}_{int} = \begin{cases} \frac{f}{m_\rho} \bar{\psi}^\mu \gamma^\nu \psi F_{\mu\nu} & \text{for } J^\pi = \frac{3}{2}^- \\ \frac{f}{m_\rho} \bar{\psi}^\mu \gamma^5 \gamma^\nu \psi F_{\mu\nu} & \text{for } J^\pi = \frac{3}{2}^+ \\ \frac{f}{m_\rho} \bar{\psi} \gamma^5 \sigma^{\mu\nu} \psi F_{\mu\nu} & \text{for } J^\pi = \frac{1}{2}^- \\ \frac{f}{m_\rho} \bar{\psi} \sigma^{\mu\nu} \psi F_{\mu\nu} & \text{for } J^\pi = \frac{1}{2}^+ \end{cases} . \quad (14)$$

Here ψ^μ denotes the resonance spinor and ψ the nucleon spinor, $\sigma^{\mu\nu} = \frac{i}{2} [\gamma^\mu, \gamma^\nu]$ and $F^{\mu\nu} = \partial^\mu \rho^\nu - \partial^\nu \rho^\mu$. We note in passing that from these Lagrangians the non-relativistic expressions from our previous publication [10] are readily obtained. We require gauge invariant interactions in order to ensure physical results in the vicinity of the photon point $q^2 = 0$.

The coupling of spin-1 particles to the baryon resonances is not uniquely determined by its quantum numbers. In analogy to the commonly used couplings for the $\Delta N \gamma$ system, we employ – in addition to the couplings in Eq. 14 – the following couplings in the p -wave channel (see for comparison e.g. [27, 28]):

$$\mathcal{L}_{int} = \begin{cases} \frac{f}{m_\rho^2} \bar{\psi}^\mu \gamma^5 \partial^\nu \psi F_{\mu\nu} \\ \frac{f}{m_\rho^2} \bar{\psi}^\mu \gamma^5 \psi \partial^\nu F_{\mu\nu} \end{cases} . \quad (15)$$

In general, the dimensionless coupling constant f is different in all three cases. For resonances with negative parity, the corresponding Lagrangians \mathcal{L}_{int} can be obtained by dropping the γ^5 -matrix. In Sect. 6 we will explore the sensitivity of the resonance model on the chosen vertex function. For the comparison between non-relativistic and relativistic calculation in Sect. 5 the coupling from Eq. 14 will be employed.

In view of the difficulties in constructing a relativistic theory for spin- $\frac{5}{2}$ fields, we treat them non-relativistically. In the relevant kinematical region only resonances with positive parity couple sufficiently to the ρN system. We can therefore restrict ourselves to the discussion of p -wave channels. In agreement with previous studies [9, 10] the following Lagrangian is used:

$$\mathcal{L}_{int} = \frac{f}{m_\rho} \chi_R^\dagger R^{ij} F_{ij} \chi \quad . \quad (16)$$

Here χ_R^\dagger and χ are resonance and nucleon spinor. R^{ij} denotes the spin- $\frac{5}{2}$ transition operator [9]. We will come back to the treatment of spin- $\frac{5}{2}$ particles in Sect. 5 and Sect. 6.

For the isospin coupling we take the standard form:

$$\begin{aligned} \chi_R^\dagger \sigma_k \rho_k \chi & \text{ for } I = \frac{1}{2} \\ \chi_R^\dagger S_k \rho_k \chi & \text{ for } I = \frac{3}{2} \end{aligned} \quad . \quad (17)$$

χ_R and χ denote resonance and nucleon isospinor, respectively, S_k is the isospin- $\frac{3}{2}$ transition operator and σ_k the standard Pauli matrix.

In the actual calculation each vertex is multiplied by a phenomenological formfactor [27]:

$$F(s) = \frac{\Lambda^4}{\Lambda^4 + (s - m_R^2)^2} \quad . \quad (18)$$

This formfactor is Lorentz invariant and has its maximum at $s = m_R^2$. For the cutoff parameter we take a value of $\Lambda = 1$ GeV for all resonances, in accordance with [27]. This formfactor has a very different functional dependence compared to the one previously used in the non-relativistic treatment:

$$F(\mathbf{q})_{old} = \sqrt{\frac{\Lambda^2}{\Lambda^2 + \mathbf{q}^2}} \quad . \quad (19)$$

The influence of the new formfactor on the results will be discussed in Sect. 5.

3.1 The Resonance Propagator

In this Section we discuss the propagator of the formed baryon resonance. A proper description of this quantity is not a trivial task since it displays in general – already in the spin- $\frac{1}{2}$ sector – a very rich spinor structure (see e.g. [29]). We show that a commonly used recipe for both the propagators of spin- $\frac{1}{2}$ and spin- $\frac{3}{2}$ particles [30, 31] leads to unphysical results in the case of ρN scattering. Then we derive an improved propagator which – albeit being only a crude approximation of the exact solution – is nonetheless sufficient for our purposes.

Unitarity relates the matrix element for the decay of a resonance R into a nucleon and a ρ meson of given polarization $|\mathcal{M}_{RN\rho}^{T/L}|^2$ to the imaginary part of the ρN forward scattering amplitude $T^{T/L}$:

$$\begin{aligned} \text{Im } T^{T/L} &\sim \sigma_{\rho N}^{tot} \\ &\sim \Gamma_{\rho} \Gamma_{tot} \\ &\sim |\mathcal{M}_{RN\rho}^{T/L}|^2 \quad . \end{aligned} \tag{20}$$

It may be objected that for tree-level calculations unitarity is by no means guaranteed [33]. However by considering only the contribution of one resonance in the s -channel, unitarity can be fulfilled provided that the decay width and the resonance propagator are parametrized in a consistent way.

Let us start with the calculation of the squared matrix element for the resonance decay $|\mathcal{M}_{RN\rho}^{T/L}|^2$. This calculation involves the completeness relation of the resonance spinor. Taking it naively as

$$\sum_r u_r^R(k) \bar{u}_r^R(k) = \not{k} + m_R \tag{21}$$

even for resonances off the mass-shell, i. e. with $\sqrt{k^2} \neq m_R$, leads to negative values for the squared matrix element. This is demonstrated in the Appendix. Thus, Eq. 21 is not appropriate in the off-shell case and needs to be modified. The obvious choice is to set [34, 35]

$$\sum_r u_r^R(k) \bar{u}_r^R(k) = \not{k} + \sqrt{k^2} \quad . \tag{22}$$

Unitarity now enforces that the modified completeness relation Eq. 22 also changes the functional dependence of the (imaginary part of the) propagator. For a spin- $\frac{1}{2}$ particle one thus obtains

$$D_{\frac{1}{2}}(k) = \frac{\not{k} + \sqrt{k^2}}{k^2 - m_R^2 + i\sqrt{k^2} \Gamma} \tag{23}$$

instead of

$$D_{\frac{1}{2}}^{trial}(k) = \frac{\not{k} + m_R}{k^2 - m_R^2 + i\sqrt{k^2} \Gamma} \quad . \tag{24}$$

The latter form is often employed in the literature [30, 31]. Since – from unitarity – it is related to the completeness relation with m_R , it leads to negative values for the total ρN cross-section $\sigma_{\rho N}^{tot}$.

In the Appendix we give some theoretical backing for Eq. 23. In particular, we show that Eq. 24 violates a fundamental constraint for the propagator and should therefore be rejected. We also discuss that Eq. 23 is only correct for the imaginary part of $D_{\frac{1}{2}}(k)$, but not for the real part. In an explicit calculation we have checked however, that the differences between the exact solution and $\text{Re } D_{\frac{1}{2}}(k)$ as taken from Eq. 23 are negligible.

The propagator $D_{\frac{3}{2}}^{\alpha\beta}(k)$ of non-interacting spin- $\frac{3}{2}$ particles is given by the well known Rarita-Schwinger propagator [36]. The conventional choice of adding a finite decay width in the denominator [31, 32] leads – as in the case of spin- $\frac{1}{2}$ particles – to negative total cross-sections for processes including intermediate $J^\pi = \frac{3}{2}^+$ resonances. As explained in the Appendix we propose therefore that the propagator should read:

$$D_{\frac{3}{2}}^{\alpha\beta}(k) = \frac{\not{k} + \sqrt{k^2}}{k^2 - m_R^2 + i\sqrt{k^2}\Gamma} \times \left[g^{\alpha\beta} - \frac{1}{3}\gamma^\alpha\gamma^\beta - \frac{2}{3}\frac{k^\alpha k^\beta}{k^2} + \frac{1}{3}\frac{k^\alpha\gamma^\beta - k^\beta\gamma^\alpha}{\sqrt{k^2}} \right]. \quad (25)$$

Some remarks about this propagator are in order. First we note that it is directly proportional to the spin- $\frac{3}{2}$ projector $P_{\frac{3}{2}}^{\alpha\beta}$, see [33]. Second, in analogy with the case of spin- $\frac{1}{2}$ resonances this expression is – strictly speaking – not correct for the real part, but again we expect the deviations to be negligible for our purposes. Finally, Eq. 25 has already been discussed in the literature [33, 30, 31]. In [30] the replacement $m_R \rightarrow \sqrt{k^2}$ is introduced to insure gauge invariance. This is not necessary in our case as the vector mesons are introduced via the gauge invariant field tensor $F^{\mu\nu}$. On the other hand, in [33] it was shown that Eq. 25 is incorrect in the limit of a small decay width Γ . This observation is in full agreement with our previous statements about the real part of Eqs. 23 and 25. Also, as pointed out in [33, 31], the propagator Eq. 25 displays a pole at $k^2 = 0$, which can lead to divergent results for scattering amplitudes. However, this kinematical regime is reached only in u -channel processes which we do not include in our model. Therefore the results of this work should not be troubled from these poles. One should

also be aware of the fact that the use of gauge-invariant couplings for the spin- $\frac{3}{2}$ field – which introduce additional orders of the resonance momentum – as suggested in [32] avoids these poles.

4 Included Resonances And Their Parameters

In this Section we list the resonances included in our model for Σ_{med} and discuss their parameters such as mass, decay width and branching ratios.

We include all baryon resonances with a sizeable coupling to the ρN channel. They are listed in Table 1. The nucleon is no longer included in the model. We found in a relativistic calculation on the T -matrix level that the Born terms lead to a strong overestimation of the data for the reactions $\gamma N \rightarrow \rho N$ and $\pi N \rightarrow \rho N$, as well as for reactions with an ω meson in the final state. It is very likely, that on this level important backscattering effects are missing, since the nucleon has a large coupling strength to the $N\pi$, $N\omega$ and $N\rho$ channels. Similar effects are known from Compton scattering, where in a K -matrix analysis the Born terms yield satisfactory results. In a T -matrix approach, additional formfactors, which suppress the contribution in backward direction, have to be introduced in an *ad-hoc* manner [37]. Therefore it does not seem appropriate to include the nucleon in our model. For resonances, on the other hand, backscattering effects are effectively taken into account by their decay width.

In contrast to our previous publication [10], we take the resonance parameters from the analysis of Manley *et al* [17, 18] rather than those from the PDG group [19]. The PDG parameters represent estimates of resonance properties, averaging the available experimental results. They are based on a variety of theoretical models, which in general differ in many details, as for example the included resonances or the treatment of the non-resonant background. Therefore, the extracted parameters are strongly model dependent and it is questionable whether an average of the results from different studies provides conclusive information on any specific reaction channel. To ensure a realistic description of the ρN scattering amplitude, it is much safer to stick to the results of a single analysis of $\pi N \rightarrow \pi\pi N$ reactions. In the work of Manley *et al* the available data set for the reaction $\pi N \rightarrow \pi\pi N$

was analyzed within an isobar model, which allows for various intermediate $\pi\pi N$ states, such as $\Delta\pi$ and $N\rho$. All partial waves were fitted with resonance plus background terms and from that fit the resonance parameters were extracted. Similar work has been done by various other groups [38]. We follow the results of Manley *et al*, since his analysis is the most extensive and recent one. In this way, rather than by using the parameters of [19], experimental information on ρN scattering enters into the model in a well defined way.

In Table 1 we list the mass m_R , the total decay width Γ_{tot} and the decay width into the ρN channel, as taken from [18]. For comparison, we also give the value for the ρN decay width from [19]. In the last column we denote if the respective resonance decays in a relative s -wave or p -wave into the ρN channel.

A considerable uncertainty in the model is connected with the coupling strength of some resonances to the ρN channel. This is most evident for transversely polarized ρ mesons. Here, at intermediate and high momenta, the $P_{13}(1720)$ resonance plays a dominant role, due to its large partial decay width into the ρN channel as given in the analysis of Manley *et al* [18]. As listed in Table 1, the estimate of the PDG group [19] is smaller by a factor of 3. Moreover, in Manley's analysis a large error of 168 MeV - which is of about the same size as the decay width itself - is stated. Similarly, for the $D_{33}(1700)$ the partial decay width as given by PDG and by Manley differ by a factor of 3, mainly affecting the results of A_ρ^L . Again, Manley gives a very large error of 31 MeV for this parameter. On the other hand, very good agreement is reached on the properties of the $D_{13}(1520)$. Here, Manley and the PDG group present nearly identical values for the partial decay width. Furthermore, the error for this number is much smaller, only 6 MeV are listed in [18].

In Manley's fit a few high lying resonances, which have not been included in our previous calculation, show a sizeable branching ratio into the ρN channel. They are listed below the double-line in Table 1. However, as will be discussed in Sect. 5, they induce only small changes on the results.

The total decay width Γ of the resonances is taken as a sum over all partial decay channels. The branching ratios into these channels as well as the mass dependence of the decays are the same as in [18], except for the ρN decay. This decay channel is calculated within the same framework as the forward scattering amplitude, see Eq. 8.

Due to the small phase space there is no measured decay width of the $P_{33}(1232)$ into ρN . Therefore the coupling constant of this resonance to the ρN system can not be obtained by a fit to the decay width and is subject to substantial uncertainty. In our previous calculation, as well as in other works [15, 16], it was taken from the Bonn potential model. It is however questionable, whether this value has much meaning outside the Bonn model (cf. discussion in [39]). We therefore calculate the coupling constant directly from the well known isovector part of the $\Delta \rightarrow N \gamma$ decay width, assuming the validity of strict VMD [40]. Note that the numerical values obtained in both ways are nearly identical. The mass dependence of the decay width is obtained in the same way as for the other resonances.

It might be argued, that the consistency of the resonance parameters employed for the calculation of the ρN forward scattering amplitude can be tested by comparing with data on the reaction $\pi N \rightarrow \rho N$ [41]. On inspection of these data, there seems to be a lack of strength below the threshold at roughly 1.7 GeV, in conflict with a large coupling of the $D_{13}(1520)$. However, this conclusion is not correct. The ρN “data points” were extracted from the measured $\pi \pi N$ data by simple fits of the mass differential cross section. Naturally, with such a procedure no sensitivity is achieved in the subthreshold region, where the ρ meson can not directly be identified from the $\pi \pi$ mass spectrum. Such a fit is certainly much less conclusive than the partial wave analysis of Manley *et al.* Moreover, the data set used by Manley *et al* also comprises the $\pi N \rightarrow \pi \pi N$ data from [41].

5 Results 1 - Relativistic Versus Non-Relativistic

In Sect. 2.2 we discussed the shortcomings of the non-relativistic calculation of the self energy Σ^{med} of the ρ meson. We then developed the framework for a fully relativistic calculation. Now we compare the non-relativistic and the relativistic approach and pay special attention to the question, whether a reference frame exists, in which the non-relativistic reduction should be performed in order to arrive at a good approximation of the relativistic results.

In a resonance model, neglecting level repulsion for the moment, the spectral function A_ρ is most sensitive to the behaviour of the scattering

amplitude in the vicinity of $s = m_R^2$, i.e. along the lines depicted in Fig. 3. In order to get a feeling for the differences between a relativistic and the different non-relativistic descriptions, it is therefore rewarding to compare the results from both approaches for the quantity $\Omega^{T/L}$, which relates to the forward scattering amplitude as:

$$T^{T/L} = -\frac{\Omega^{T/L}}{k^2 - m_R^2 + i\sqrt{k^2}\Gamma} \quad . \quad (26)$$

Here k^2 stands for the invariant mass of the ρN system. Note that the coupling constants f are already adjusted to the partial decay width of the resonance.

In Fig. 4 we show Ω^T for two of the most prominent resonances in the non-relativistic analysis, the $D_{13}(1520)$ and the $P_{13}(1720)$. It is plotted as a function of the invariant mass of the ρ meson, the momentum being fixed by the condition $s = m_R^2$. We compare the relativistic results with three non-relativistic versions of Σ^{med} , which are explained in detail in Sect. 2.2:

- i) relativistic
- ii) non-relativistic, selfenergy lab-frame, coupling constant cm-frame
- iii) non-relativistic, both quantities cm-frame
- iv) non-relativistic, both quantities lab-frame .

Up to now, in the literature only calculations performed within kinematics ii) can be found [10, 9, 15].

We first remark that the results are not degenerate at threshold, since in each case the coupling constant has been adjusted to the measured partial decay width. As expected from the discussion in Sect. 2.2, the calculations reveal large differences between the different non-relativistic approaches ii)-iv) in the transverse channel. This effect is – as already discussed – more pronounced for p -wave resonances, see lower graph of Fig. 4. Here, especially at low invariant masses, the commonly used non-relativistic version ii) is not reliable at all, overestimating the results by a factor of 2 – 3, whereas both version iii) and iv) yield a surprisingly good agreement with the fully relativistic calculation i). In the s -wave channel – upper graph of Fig. 4 –

it is again the non-relativistic version ii) displaying a considerable disagreement with the relativistic calculation. Both versions iii) and iv) yield better approximations. The exact form of the momentum dependence, however, is not well reproduced in version iv).

We do not show results for Ω^L . Here the effect from a relativistic calculation is rather small, since the momentum dependence of Ω^L is mainly determined from physical constraints at $\mathbf{q} = 0$ and at the photon point: at small momenta a relativistic calculation and its non-relativistic reduction must display a similar behaviour, whilst at the photon point Ω^L has to vanish in either version. Thus, both calculations do not have much room to develop differently. There is a finite contribution to Ω^L from p -wave resonances, which, however, is small as compared to the transverse coupling. In the spin- $\frac{1}{2}$ sector, one obtains qualitatively similar results for $\Omega^{T/L}$.

Summarizing these results, we find that the previously used non-relativistic version ii) is not a good approximation of a fully relativistic calculation. In contrast, using cm-kinematics for both the determination of the coupling constant and the self energy leads to a very reasonable agreement with the relativistic approach.

For this reason we argue also that the contribution from spin- $\frac{5}{2}$ particles — for which a relativistic theory is very complicated — should be evaluated within kinematics iii). Since in a non-relativistic calculation the vertex factors of both the spin- $\frac{3}{2}$ and spin- $\frac{5}{2}$ resonances are proportional to \mathbf{q}^2 , we expect from Fig. 4 that at high momenta the contribution from spin- $\frac{5}{2}$ resonances is reduced as compared to previous works [9, 10, 15], where \mathbf{q}^2 was evaluated in the lab-frame.

Turning now to the discussion of the results for the spectral function, we start with a comparison between a relativistic calculation and the non-relativistic approach with kinematics iii). The good agreement for the results of $\Omega^{T/L}$ translates into very similar results for the spectralfunction $A_\rho^{T/L}$, see Fig. 5. There the transverse spectralfunction is plotted at momenta $q = 0$ GeV and $q = 0.8$ GeV. The resonance parameters are taken from Manley *et al*, only the resonances above the double line in Table 1 are included. The small deviations at large momenta are partly due to the different choices for the formfactor, see Eqs. 18 and 19. The effect of the formfactor will be discussed in more detail later on in this Section. We do not present a comparison for the longitudinal channel as there the differences are even smaller.

Since the agreement between these two approaches is nearly perfect we will use the remainder of this Section for the comparison of our previous non-relativistic results (within kinematics *ii*) and the relativistic ones. Differences between both versions are not only due to kinematics. Also the changes in the resonance parameters and the influence of the new formfactor need to be considered. This is apparent already at low momenta, see Fig. 6. For the moment we concentrate on a comparison of our previous non-relativistic calculation (dotted line) with the relativistic one, where the same resonances as in the non-relativistic case (listed above the double-line in Table 1) are included (dashed line). At $\mathbf{q} = 0$ the non-relativistic calculation with PDG parameters shows a stronger depletion of the ρ peak than the relativistic approach with Manley's parameters. The formfactor $F(s)$ (18) suppresses off-shell contributions ($s \neq m_R^2$) of resonances much stronger than the previously used one (19). This effects in general both the tail of the resonance excitation as, due to level repulsion, the strength in the resonance peak. Thus, due to the formfactor, the impact of the excitation of the $D_{13}(1520)$ in the region of the ρ peak is noticeably reduced. This effect is enhanced by the small partial ρN decay width of the $D_{33}(1700)$ found in the Manley analysis as compared to PDG (ct. Table 1). Its small coupling makes this resonance play a merely negligible role in the relativistic calculation.

At larger momenta both approaches lead to very different results for A_ρ^T , see Fig. 7. As a general tendency, much more strength is centered around the original ρ peak. This behaviour can be retraced to various sources. As follows from the properties of $\Omega^{T/L}$, for a given branching ratio, a relativistic calculation produces a much smaller Σ_{med}^T than a non-relativistic one. The resonance contribution is further suppressed by the formfactor $F(s)$, thus producing a more conservative estimate of the resonance contribution. In addition, at higher momenta, Σ_{med} is reduced by the smaller branching ratio of the $D_{33}(1700)$. These depletion mechanisms are only counteracted by the strongly increased branching ratio of the $P_{13}(1720)$. Overall, at high momenta A_ρ^T is dominated by the $D_{13}(1520)$ and the $P_{13}(1720)$ as well as, to some extent, by the spin- $\frac{5}{2}$ resonances $F_{15}(1680)$ and $F_{35}(1905)$. Still the transverse spectral function receives significant broadening with increasing 3-momentum in a relativistic calculation, but this effect is not as pronounced as in the non-relativistic case.

Whereas A^T receives strong qualitative modifications in a relativistic calculation, changes in A^L are only of a quantitative nature. This is shown

in Fig. 8. As already mentioned, the momentum dependence is dominated — both in a relativistic and a non-relativistic approach — by physical constraints at $\mathbf{q} = 0$ and $q^2 = 0$. Consequently, the $D_{13}(1520)$ peak at $\mathbf{q} = 0.4$ GeV contains nearly the same strength in both approaches. The depletion of resonance strength around the ρ peak is, as in the case of $\mathbf{q} = 0$, due to the formfactor and the small coupling of the $D_{33}(1700)$. In the longitudinal channel the only sizeable contribution comes from the $D_{13}(1520)$.

The impact of the new, high lying resonances on our results is small and noticeable only at high momenta. This is easily understood for the following reasons: Despite their large branching ratio, the coupling strength is relatively small, since their mass is far above the ρN threshold and consequently the phase space is very large. In addition, they have a very large total decay width, leading to a further suppression of the contribution. At low momenta, these resonances can only be excited from ρ mesons far above their pole mass. Correspondingly, their contribution to the imaginary part of Σ_{med} is drowned by the imaginary part of the vacuum self energy, the 2π decay width. It is only at momenta around 0.8 GeV, that the resonance excitation occurs at invariant masses around the pole mass of the ρ meson. At this point resonance scattering becomes important. This is shown in Figs. 6-8, where the calculation including all resonances is represented by the solid line.

Finally, we discuss the effect of medium modifications of the scattering amplitude. The Fermi averaging shows sizeable impact only at large momenta, leading to a broadening of the resonance peaks. As for the case of Fermi averaging, short range correlations influence the results mostly at high momenta. We show a comparison of the influence of both modifications on A_ρ^T at $\mathbf{q} = 0.8$ GeV in Fig. 9. For A_ρ^L the differences are completely negligible.

6 Results 2 - Influence of Couplings

So far, we discussed the differences between a relativistic and a non-relativistic calculation of Σ_{med} and their consequences for A_ρ . There are, in addition, various ways for a resonance to couple to the ρN system. In order to draw safe conclusions on the momentum dependence of the ρN scattering amplitude, it is important to study the influence of the chosen coupling on the results.

In this analysis we confine ourselves to the case of spin- $\frac{3}{2}$ resonances of

both positive and negative parity. The vertex functions are derived from the Lagrangians in Eqs. 14 and 15. In the spin- $\frac{1}{2}$ sector there is no resonance which has a sizeable coupling to ρN . Clearly, a strong dependence of the final results on the coupling of spin- $\frac{1}{2}$ resonances is not expected.

In the following discussion we will use some shorthand notations to distinguish between the different vertex functions. The standard coupling from Eq. 14 will be referred to as coupling (i), to the first vertex function from Eq. 15 we refer as coupling (ii) and to the second one as coupling (iii). To get a feeling for the changes, we present first $\Omega^{T/L}$ in Fig. 10 and 11. The results are shown for the $D_{13}(1520)$ and the $P_{13}(1720)$ resonances. Note that the coupling constants f are already adjusted to the ρN branching ratios. The most distinct behaviour is exhibited by coupling (iii). At the photon point, it enforces a vanishing contribution not only in the longitudinal, but also in the transverse channel. This behaviour can be read off from the Lagrangian \mathcal{L}_{int} :

$$\partial^\nu F_{\mu\nu} = -q^2 A^\nu \quad . \quad (27)$$

Clearly, the vertex function has to vanish at $q^2 = 0$, regardless of the polarization of the ρ meson. Consequently, Σ_{med}^T has to fulfill the same constraints as Σ_{med}^L . Both become more or less identical. Thus, the coupling (iii) mostly affects the transverse channel. Noteworthy is also the much larger contribution from p -wave resonances to Ω^L .

For the same ρN branching ratios, large coupling constants are obtained by using coupling (iii), as compared to the other two couplings schemes. In the determination of the coupling strength the quantity $2\Omega^T + \Omega^L$ enters, averaged over the ρ mass distribution. Since this expression has to vanish at $q^2 = 0$ in coupling (iii), its size is much reduced at low invariant masses. This behaviour can only be compensated by a large coupling constant. For p -wave resonances this effect is most evident, since in this case the matrix element becomes sizeable mostly near the photon point for the couplings (i) and (ii). As an example, we obtain a value of $f = 36$ for the $P_{13}(1720)$ in coupling (iii) as compared to $f = 10$ in coupling (i). Clearly, the increased values for the coupling constants are responsible for the enhanced resonance contribution in the longitudinal channel.

For coupling (iii) the coupling strength for the $P_{33}(1232)$ can not be obtained from VMD since the matrix element vanishes at the photon point.

We take an *ad hoc* value of $f = 30$ for the coupling constant, which is twice as much as obtained from coupling (i). Varying f between values of 15 – 30 has only negligible influence on the results.

Coupling (ii) produces much less dramatic changes as compared to (iii). The general properties of $\Omega^{T/L}$ do not change much in comparison to a calculation employing coupling (i). An exception is the coupling of p -wave resonances to longitudinal ρ mesons, where coupling (ii) generates a much larger contribution than coupling (i). Quantitatively, also the coupling of s -wave resonances to transverse ρ mesons change up to some extent. Nearly identical results are achieved in the remaining channels.

Turning now to the results for the spectral function, at $\mathbf{q} = 0$ no significant modification is observed, see Fig. 12. However, at higher momenta, the distinct character of coupling (iii) becomes apparent, reducing the resonance contribution at low invariant masses for transverse ρ mesons. At the same time, a stronger modification of A^L is exhibited. Thus, coupling (iii) induces a qualitatively different behaviour on A_ρ , removing much of the distinction between transverse and longitudinal ρ mesons. The results at high momenta are shown in Fig. 13. In this kinematical region spin- $\frac{5}{2}$ resonances, for which we have only a non-relativistic coupling at hand, have noticeable influence on the results. Therefore, by changing the interaction in the spin- $\frac{3}{2}$ sector and leaving the spin- $\frac{5}{2}$ sector unchanged, the effect of the coupling scheme on the spectral function is underestimated. In order to obtain an upper limit for this effect, we treat the spin- $\frac{5}{2}$ resonances the same way as spin- $\frac{3}{2}$ resonances, correcting for the different spins of the states by a factor of 3/2. This procedure is reasonable, since — except for the multiplicity — the spin of the resonance affects mostly the angular dependence of the matrix element. We checked that for the transition from spin- $\frac{1}{2}$ to spin- $\frac{3}{2}$ resonances our prescription works fine within 10%.

The most distinct feature of coupling (ii) is an increased resonance contribution to A^L at large momenta. The transverse channel, however, does not undergo large modifications as compared to coupling (i).

One should keep in mind, that in general the actual coupling of a resonance to the ρN channel might contain contributions from all three couplings. Naturally this will smear out the differences. One expects from the above discussion, that the general tendency will go towards a less modified transverse ρ meson than predicted from coupling (i), whereas in the longitudinal channel a stronger modification is likely. It is beyond the scope

of this work, however, to find realistic weighting factors for each coupling. This can only be achieved by a complete relativistic partial wave analysis of $\pi N \rightarrow \pi \pi N$ data.

7 Conclusions

We have performed a calculation of the ρ spectral function A_ρ in nuclear matter within a relativistic resonance model. The aim was, to put predictions concerning the properties of ρ mesons in nuclear matter, which were derived in a non-relativistic reduction [10], on a more solid basis. Especially the momentum dependence of A_ρ was examined. This discussion was motivated by the observation that the results of a non-relativistic calculation depend strongly on the reference frame in which the non-relativistic vertex functions are evaluated. We also investigated the influence of different resonance parameters. We argued, that the resonance parameters as obtained in the work of Manley *et al* [17, 18] provide much more reliable information on ρN scattering than the estimated resonance parameters listed in PDG [19]. Finally, we studied if and to which extent the obtained results depend on the structure of the chosen coupling. Therefore, various coupling schemes for the $RN\rho$ vertex were employed in the spin- $\frac{3}{2}$ sector.

A very interesting finding of this work is that a non-relativistic approach is in very good agreement with a relativistic one and should be good enough for all practical purposes, provided that the vertex functions for both the determination of the coupling constant and the scattering amplitude are evaluated in the cm-frame, i.e. the rest frame of the intermediate resonance. In contrast, it is not advisable to determine the coupling constant with cm-kinematics but the scattering amplitude in the rest frame of the nucleon, as was done in all previous works [9, 10, 15, 16]. We could demonstrate that this procedure leads to dramatic deviations from a relativistic calculation.

As an important finding in our previous non-relativistic calculation, we reported on the dominant role of the $D_{13}(1520)$ in ρN scattering. At low momenta these results are supported by the relativistic calculation. The parameters of this resonance are well known. Furthermore, different vertex functions show only marginal effects on the results. For higher momenta the role of the $D_{13}(1520)$ is reduced in a relativistic calculation.

Another striking outcome of a non-relativistic calculation was the very dif-

ferent behaviour of A_ρ^T and A_ρ^L at high momenta. In the light of a relativistic version of A_ρ this distinction needs to be revised. As an overall effect, taking into account all modifications on the calculations, a transversely polarized ρ meson gathers a larger amount of its total strength around the pole mass. The previous finding of a completely structureless strength distribution in the transverse channel at high momenta can therefore not be confirmed. In particular, the coupling with a derivative acting on the ρ field tensor produces a transverse spectral function A_ρ^T , which undergoes less modifications at high momenta and is very similar to A_ρ^L .

The reliability of the calculation in the transverse channel is limited by poorly known resonance parameters, especially their partial decay width into the ρN channel. In particular, a large uncertainty is connected with the branching ratio of the $P_{13}(1720)$. In this partial wave, experimental data do not allow a conclusive determination of the resonance parameters.

In the longitudinal channel only quantitative changes occur. Here, the results are governed by physical constraints at threshold and at the photon point. The change from a non-relativistic to a relativistic calculation has no substantial impact on the results. As in the transverse channel, at large momenta the coupling with a derivative acting on the ρ field tensor, produces the largest quantitative change. In this case it leads to a pronounced broadening of the ρ peak. Up to which extent this coupling is present in the actual $RN\rho$ vertex remains an open question. As a general tendency, it will lead to a smaller modification of the transverse channel, whereas the influence of resonance scattering for longitudinal ρ mesons is enhanced.

Altogether, we can confirm the dominant influence of the $D_{13}(1520)$ on the propagation of ρ mesons in nuclear matter at low momenta. The sensitivity to the chosen coupling scheme is small and the physical parameters of this resonance are well under control. The distinction between A_ρ^T and A_ρ^L as found in our non-relativistic study is still existent in a relativistic calculation, but only to a reduced extent.

8 Acknowledgments

The authors would like to thank W. Peters for pointing out the problems connected with the relativistic calculation of the spectral function. M.P. enjoyed many discussion with M. Effenberger concerning the Manley analysis.

A Appendix

A.1 $|\mathcal{M}_{RN\rho}^{T(L)}|^2$

In this Appendix we show the problem arising from the completeness relation Eq. 21. The squared matrix element $|\mathcal{M}_{RN\rho}^{T(L)}|^2$ for the decay of a resonance with the quantum numbers $J^\pi = \frac{1}{2}^+$ into $N\rho$ is readily calculated, using Eqs. 9, 14 and 21:

$$\begin{aligned} |\mathcal{M}_{RN\rho}^T|^2 &= -\frac{P_{\mu\nu}^T}{2} \text{Tr} \left[(\not{p}_N + m_N) \mathcal{V}_{\frac{1}{2}}^\mu (\not{k} + m_R) \mathcal{V}_{\frac{1}{2}}^\nu \right] \\ &= 4 I_\Gamma \left(\frac{f_{RN\rho}}{m_\rho} \right)^2 m_N \left(\omega^2 (m_N + \omega - m_R) + \mathbf{q}^2 (m_N + m_R - \omega) \right) \end{aligned} \quad (28)$$

$$\begin{aligned} |\mathcal{M}_{RN\rho}^L|^2 &= -P_{\mu\nu}^L \text{Tr} \left[(\not{p}_N + m_N) \mathcal{V}_{\frac{1}{2}}^\mu (\not{k} + m_R) \mathcal{V}_{\frac{1}{2}}^\nu \right] \\ &= 4 I_\Gamma \left(\frac{f_{RN\rho}}{m_\rho} \right)^2 m_N q^2 (m_N + \omega - m_R) \quad . \end{aligned}$$

The calculation is done in the rest frame of the nucleon, and I_Γ denotes an isospin factor, see Eq. 17. One easily verifies that $|\mathcal{M}_{RN\rho}^{T/L}|^2$ can become negative. At $\mathbf{q} = 0$, for example, the squared matrix element changes sign at $\omega = m_R - m_N$. Clearly, using Eq. 22 instead of Eq. 21 does not lead to such a pathological behaviour. We note in passing that for resonances with negative parity we do not find such effects.

A.2 The Propagator

According to [42] the propagator $D_{\frac{1}{2}}(k)$ has to satisfy a number of constraints. Expressing the propagator in a Lehmann representation:

$$D_{\frac{1}{2}}(k) = \int_0^\infty dM^2 \left[k \rho_{sp}(M^2) + M \rho_{sc}(M^2) \right] \frac{1}{k^2 - M^2 + i\epsilon} \quad , \quad (29)$$

these constraints translate into properties of the spinor and scalar spectral weight functions of the propagator, ρ_{sp} and ρ_{sc} respectively:

$$\begin{aligned}
\text{i)} \quad & \rho_{sp}(M^2) \text{ and } \rho_{sc}(M^2) \text{ are both real} \\
\text{ii)} \quad & \rho_{sp}(M^2) > 0 \\
\text{iii)} \quad & \rho_{sp}(M^2) - \rho_{sc}(M^2) \geq 0 \quad .
\end{aligned} \tag{30}$$

It is now possible to check whether the often used expression from Eq. 24 is compatible with these conditions. The comparison of Eqs. 24 and 29 allows the identification of the functions ρ_{sp} and ρ_{sc} :

$$\begin{aligned}
\rho_{sp}^{trial}(k^2) &= \frac{1}{\pi} \frac{\sqrt{k^2} \Gamma}{(k^2 - m_R^2)^2 + k^2 \Gamma^2} \\
\rho_{sc}^{trial}(k^2) &= \frac{1}{\pi} \frac{m_R \Gamma}{(k^2 - m_R^2)^2 + k^2 \Gamma^2} \\
&= \rho_{sp}^{trial}(k^2) \frac{m_R}{\sqrt{k^2}} \quad .
\end{aligned} \tag{31}$$

Clearly ρ_{sp}^{trial} and ρ_{sc}^{trial} , as obtained from Eq. 24, violate the last condition in Eq. 30 for $k^2 < m_R^2$.

In order to construct a more reasonable propagator which incorporates the constraints from Eq. 30, we will choose the spectral weight functions such that they fulfill these constraints and then calculate the full propagator directly from Eq. 29. Keeping things as simple as possible we make the following *ansatz* for ρ_{sp} and ρ_{sc} :

$$\rho_{sp} = \rho_{sc} = \rho_{sp}^{trial} \quad . \tag{32}$$

This is readily done for the imaginary part of the propagator, leading to the expression:

$$\text{Im } D_{\frac{1}{2}}(k) = \text{Im} \left(\frac{k + \sqrt{k^2}}{k^2 - m_R^2 + i \sqrt{k^2} \Gamma} \right) \quad . \tag{33}$$

For the real part of $D_{\frac{1}{2}}(k)$, the integral can be solved analytically only, if a constant decay width Γ is assumed, leading to a lengthy expression. Taking

into account the mass dependence of the decay width makes a numerical computation mandatory. Concerning the calculation of the ρ meson self energy we checked by explicit comparison that the *ansatz*

$$\text{Re } D_{\frac{1}{2}}(k) = \text{Re} \left(\frac{\not{k} + \sqrt{k^2}}{k^2 - m_R^2 + i \sqrt{k^2} \Gamma} \right) \quad (34)$$

produces a satisfactory agreement with the exact numerical solution. Small deviations can be seen, but these have virtually no effect on the spectral function of the ρ meson. Obviously, Eqs. 33 and 34 lead back to our guess Eq. 23.

One can write down a Lehmann representation for the propagator of spin- $\frac{3}{2}$ particles $D_{\frac{3}{2}}^{\alpha\beta}(p)$ in a straightforward extension of Eq. 29. This expression contains in principle eight spectral weight functions, four multiplying the spinor part of $D_{\frac{3}{2}}^{\alpha\beta}(p)$ and four its scalar part. By analogy to the case of spin- $\frac{1}{2}$ fields, we require them to be identical and put them equal to ρ_{sp}^{trial} from Eq. 31. Thus, we obtain the result from Eq. 25.

References

- [1] V. Koch, Int. J. Mod. Phys. **E6** (1997) 203.
- [2] J. I. Kapusta and E. V. Shuryak, Phys. Rev. **D49** (1994) 4694.
- [3] R. Pisarski, Phys. Rev. **D52** (1995) R3773.
- [4] G. Chanfray, J. Delorme and M. Ericson, Nucl. Phys. **A637** (1998) 412.
- [5] G.E. Brown and M. Rho, Phys. Rev. Lett. **66** (1991) 2720.
- [6] T. Hatsuda and S. H. Lee, Phys. Rev. **C46** (1992) R34 ; T. Hatsuda, S. H. Lee and H. Shiomi, Phys. Rev. **C52** (1995) 3364.
- [7] S. Leupold, U. Mosel, Phys. Rev. **C58** (1998) 2939 ; S. Leupold, W. Peters, U. Mosel, Nucl. Phys. **A628** (1998) 311.
- [8] B. Friman, e-Print Archive: nucl-th/9801053, Talk given at APCTP Workshop on Astro-Hadron Physics: Properties of Hadrons in Matter,

Seoul, Korea, 25-31 Oct 1997 ; B. Friman, M. Lutz and G. Wolf, e-print Archive: nucl-th/9811040, *Proceedings of the 8th International Conference on the Structure of Baryons*, Editors: D. W. Menze, B. Ch. Metsch, World Scientific, 1999.

- [9] B. Friman and H.J. Pirner, Nucl. Phys. **A617** (1997) 496.
- [10] W. Peters, M. Post, H. Lenske, S. Leupold and U. Mosel, Nucl. Phys. **A632** (1998) 109.
- [11] B. Friman, Acta Phys.Polon. **B29** (1998) 3195.
- [12] F. Klingl, N. Kaiser and W. Weise, Nucl. Phys. **A624** (1997) 527.
- [13] G. Chanfray and P. Schuck, Nucl. Phys. **A545** (1992) 271c ; Nucl. Phys. **A555** (1993) 329.
- [14] M. Herrmann, B. Friman and W. Nörenberg, Nucl. Phys. **A545** (1992) 267c ; Nucl. Phys. **A560** (1993) 411.
- [15] R.Rapp, G. Chanfray and J. Wambach, Nucl. Phys. **A617** (1997) 472.
- [16] M. Urban, M. Buballa, R. Rapp and J. Wambach, Nucl. Phys. **A641** (1998) 433.
- [17] D.M. Manley, R. A. Arndt, Y. Goradia and V. L. Teplitz, Phys. Rev. **D30** (1984) 904.
- [18] D.M. Manley and E.M. Saleski, Phys. Rev. **D45** (1992) 4002.
- [19] Particle Data Group, Phys. Rev. **D54** (1996) 1.
- [20] G. Agakichiev et al., CERES collaboration, Phys. Rev. Lett. **75** (1995) 1272.
- [21] A. Drees for the CERES collaboration, in Proc. of the International Workshop XXV on QCD Phase Transitions, Hirschegg 1995, eds. H.Feldmeier et al., (GSI Darmstadt 1997), p. 178.
- [22] N. Maseru for the HELIOS-3 collaboration, Nucl. Phys. **A590** (1995) 93c.

- [23] G. Q. Li, C. M. Ko, G. E. Brown and H. Sorge, Nucl. Phys. **A611** (1996) 539 ; E. L. Bratkovskaya, W. Cassing, R. Rapp, J. Wambach, Nucl. Phys. **A634** (1998) 168.
- [24] V. Koch and C. Song, Phys. Rev. **C54** (1996) 1903.
- [25] M. Effenberger, E L. Bratkovskaya and U. Mosel, Phys. Rev. **C60** (1999) 44614.
- [26] C. D. Dover, J. Hüfner and R. H. Lemmer, Ann. Phys. **66** (1994) 755.
- [27] T. Feuster and U. Mosel, Phys. Rev. **C58** (1998) 457.
- [28] R. M. Davidson, N. C. Mukhopadhyay and R. S.Wittman, Phys. Rev. **D43** (1991) 71.
- [29] P. A. Henning, Nucl. Phys. **A582** (1995) 633, Erratum-ibid. **A586**, 777 (1995) ; Phys. Rep. **253** (1995) 235.
- [30] R. A. Adelseck, C. Bennhold and L. E. Wright, Phys. Rev. **C32** (1985) 1681; J. C. David, C. Fayard, G. H. Lamot and B. Saghai, Phys. Rev. **C53** (1996) 2613.
- [31] I. Blomqvist and J. M. Laget, Nucl. Phys. **A280** (1977) 405; H. Garcilazo and E. Moya de Guerra, Nucl. Phys. **A562** (1993) 521; M. Schaefer, H. C. Doenges, A. Engel and U. Mosel, Nucl. Phys. **A575** (1994) 429; J. I. Johansson and H. S. Sherif, Nucl. Phys. **A575** (1994) 477.
- [32] V. Pascalutsa and R.Timmermans, Phys. Rev. **C60** (1999) 042201.
- [33] M. Benmerouche, R. M. Davidson and M. C. Mukhopadhyay, Phys. Rev. **C 39** (1989) 2339.
- [34] T. Feuster and U. Mosel, Nucl. Phys. **A612** (1997) 375.
- [35] R. Shyam, Phys. Rev. **C60** (1999) 055213.
- [36] W. Rarita, J. Schwinger, Phys. Rev. **60** (1941) 61.
- [37] T. Feuster , phd thesis at *University of Giessen*, unpublished ; T. Ishii *et al*, Nucl. Phys. **B165** (1980) 189 ; Y. Wada *et al*, Nucl. Phys. **B247** (1984) 313.

- [38] R. S. Longacre and J. Dolbeau, Nucl. Phys. **B122** (1977) 493 ; R. S. Longacre *et al*, Phys. Rev. **D17** (1978) 1795.
- [39] B. Friman and S. H. Lee, Nucl. Phys. **A653** (1999) 91.
- [40] M. Post and U. Mosel , *in preparation*.
- [41] A. D. Brody *et al* , Phys. Rev. **D4** (1971) 2693.
- [42] J. D. Bjorken and S. D. Drell, *Relativistic Quantum Fields*, McGraw-Hill International Book Company, New York, 1965. C. Itzykson and J.-B. Zuber, *Quantum Field Theory*, McGraw-Hill International Book Company, New York, 1980.

	$m_R(\text{GeV})$	$\Gamma_{tot}(\text{MeV})$	$\Gamma_{N\rho}(\text{MeV})$	$\Gamma_{N\rho}^{PDG}(\text{MeV})$	f	
$P_{33}(1232)$	1.231	118	–	–	13.9	p -wave
$D_{13}(1520)$	1.524	124	26	24	6.5	s -wave
$S_{31}(1620)$	1.672	154	44	20	2.0	s -wave
$S_{11}(1650)$	1.659	173	5	15	0.5	s -wave
$F_{15}(1680)$	1.684	139	11	12	6.46	p -wave
$D_{33}(1700)$	1.762	599	46	120	1.9	s -wave
$P_{13}(1720)$	1.717	383	333	100	10.1	p -wave
$F_{35}(1905)$	1.818	327	282	210	17.5	p -wave
P_{13}	1.879	498	217	–	3.1	p -wave
$D_{33}(1940)$	2.057	460	162	–	0.5	s -wave
$F_{15}(2000)$	1.903	494	296	–	9.5	p -wave
$D_{13}(2080)$	1.804	447	114	–	1.4	s -wave
$S_{11}(2090)$	1.928	414	203	–	0.7	s -wave

Table 1: List of the resonances included in this calculation. The parameters in the first three columns are taken from the Manley analysis [17, 18]. In the fourth column the resonance decay width into ρN as presented in the PDG [19] is listed. The fifth column shows the coupling strength of the resonances to ρN as obtained from expression (8). In the last column we denote if the respective resonance decays in a relative s -wave or p -wave into the ρN channel. The resonances below the double line have not been included in our previous analysis [10].

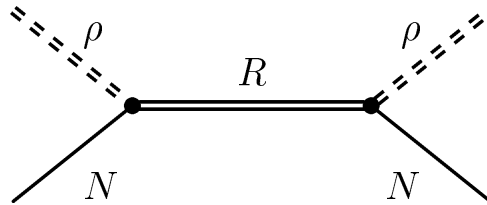


Figure 1: Contribution from a resonance to the ρN scattering amplitude.

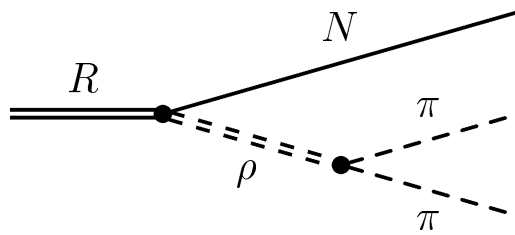


Figure 2: Decay of a resonance into two pions via an intermediate ρ meson.

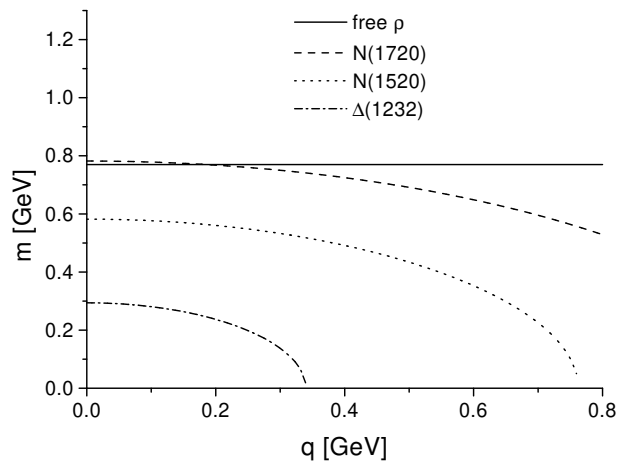


Figure 3: Free dispersion relations for the ρ and the most prominent resonances. For the resonance branches m is the invariant mass a meson of given three-momentum \mathbf{q} must have in order to excite the respective resonance on its mass shell [10].

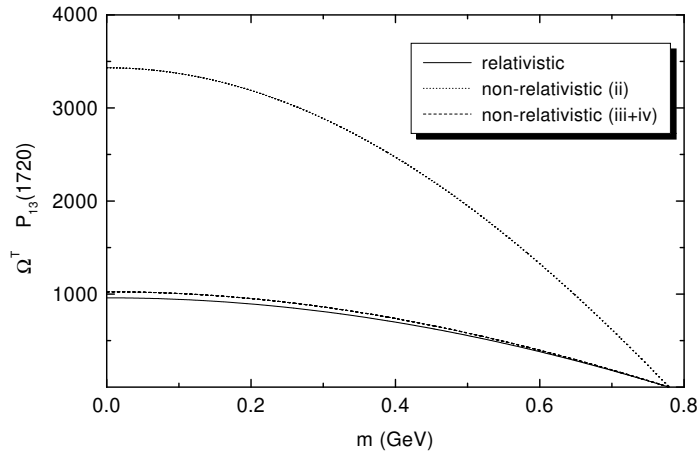
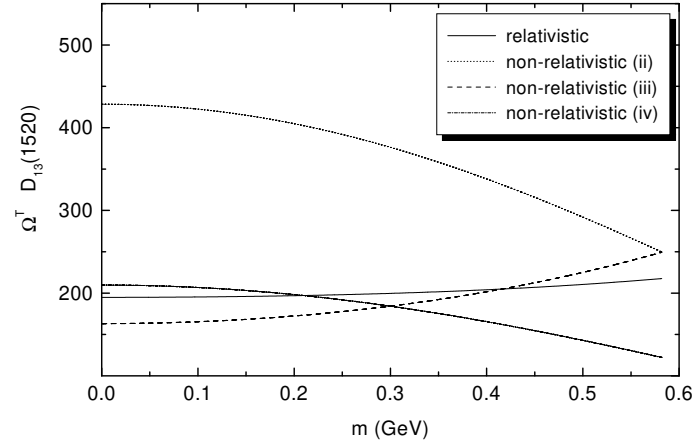


Figure 4: Ω^T for the $D_{13}(1520)$ resonance (upper graph) and the $P_{13}(1720)$ (lower graph). Shown are three different calculations, which are explained in Sect. 5.

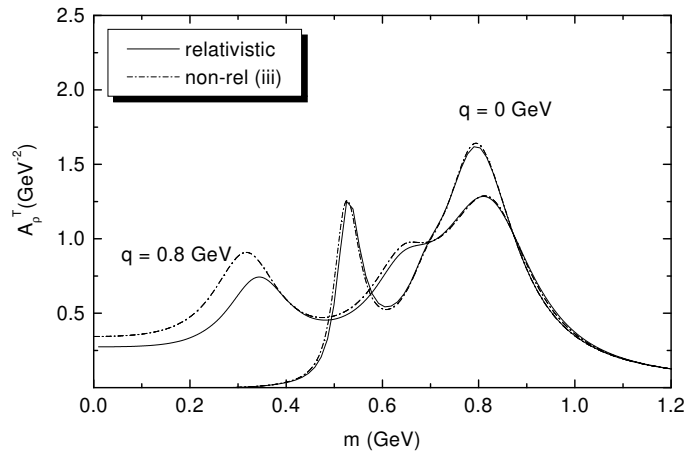


Figure 5: The transverse spectral function A_ρ^T at 0 GeV and 0.8 GeV. Shown is a comparison between a relativistic calculation and a non-relativistic one using cm-kinematics (iii).

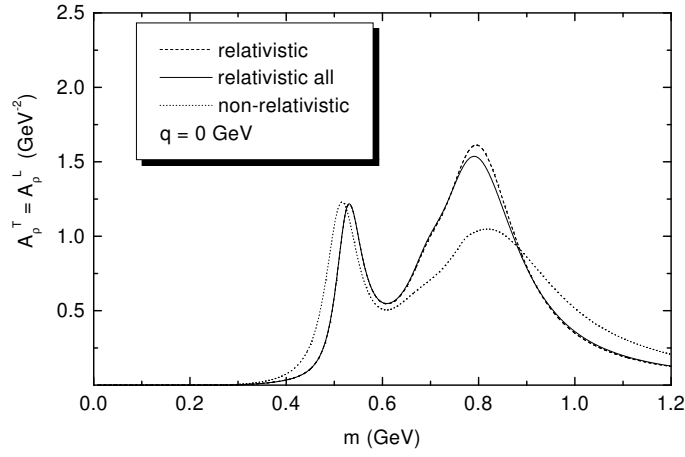


Figure 6: $A_\rho^T = A_\rho^L$ at $\mathbf{q} = 0$. Compared are a relativistic (solid line, dashed line) and a non-relativistic calculation (dotted line). For the relativistic calculation the resonance parameters of Manley *et al* [18] are employed, for the non-relativistic one the parameters of PDG [19].

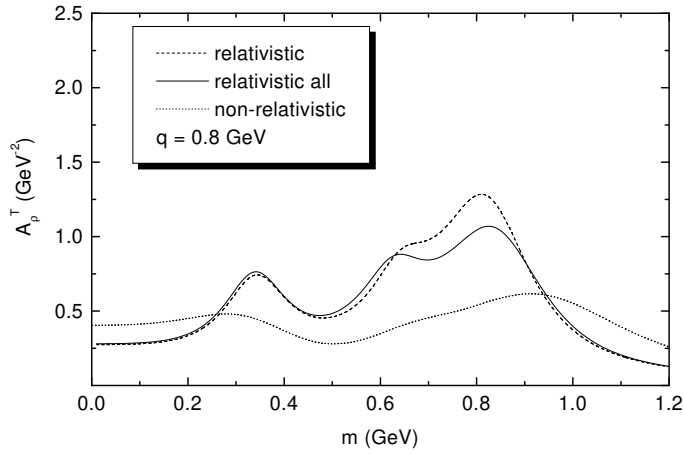
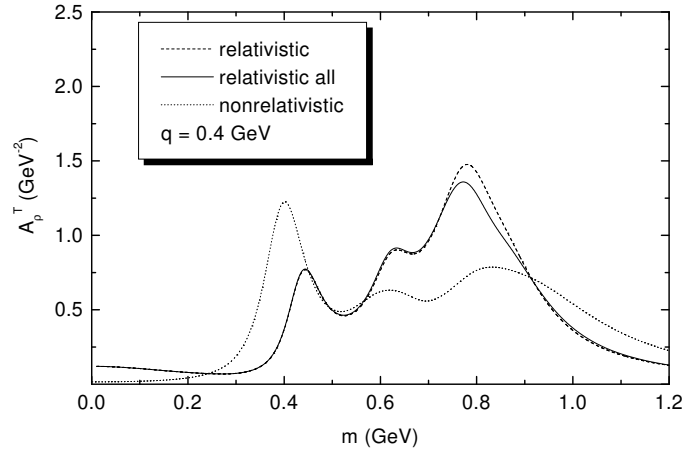


Figure 7: Same as Fig. 6 but at $\mathbf{q} = 0.4$ GeV (upper part) and at $\mathbf{q} = 0.8$ GeV (lower part).

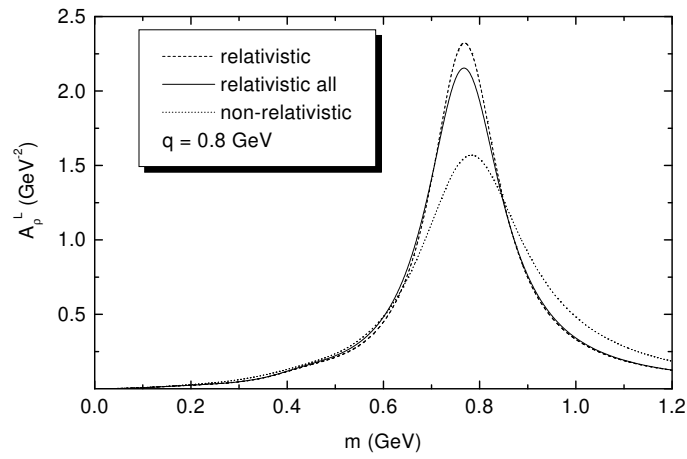
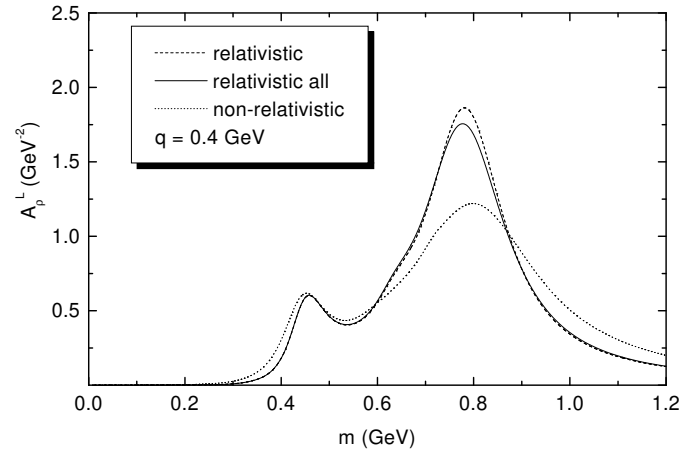


Figure 8: Same as Fig. 7, but for A_p^L .

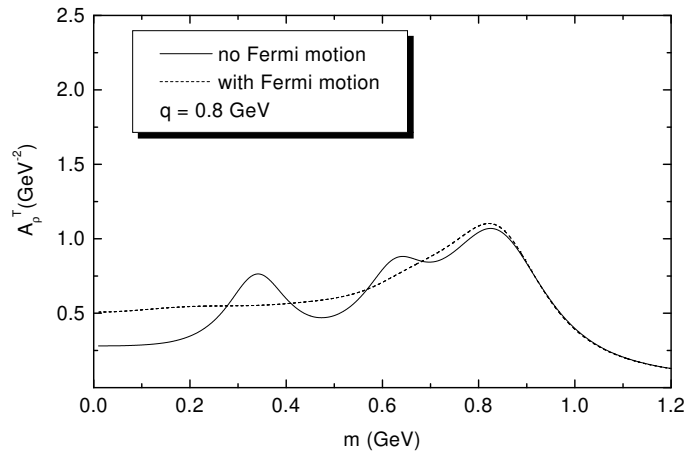


Figure 9: A_ρ^T at $\mathbf{q} = 0.8$ GeV. The vacuum result (solid line) is compared to an in-medium calculation where Fermi averaging and short range correlations are taken into account (dashed line).

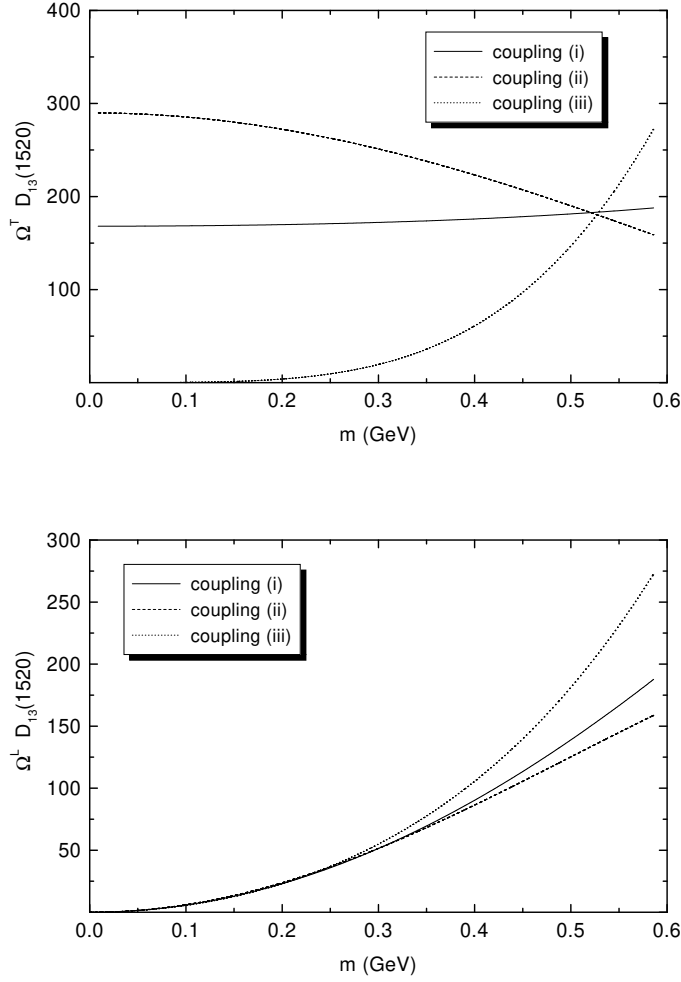


Figure 10: Ω^T (upper graph) and Ω^L (lower graph) for the $D_{13}(1520)$. Shown is the influence of different coupling schemes on the results. The couplings are explained in Sect. 6.

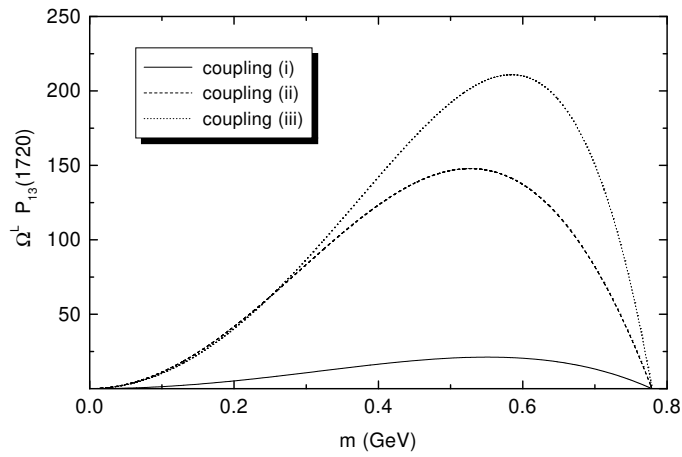
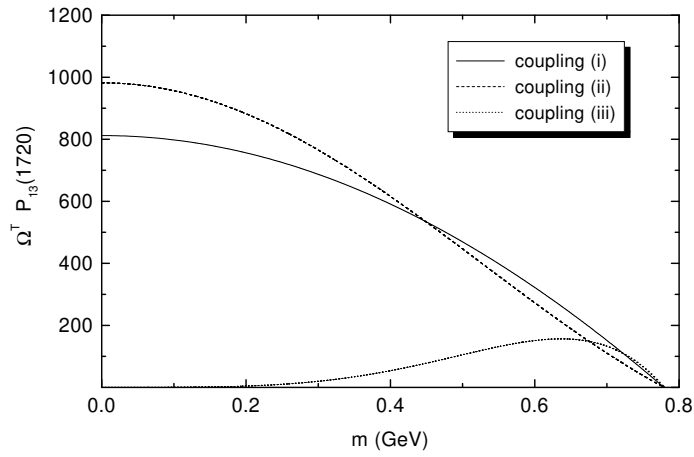


Figure 11: Same as Fig. 10 but for the $P_{13}(1720)$.

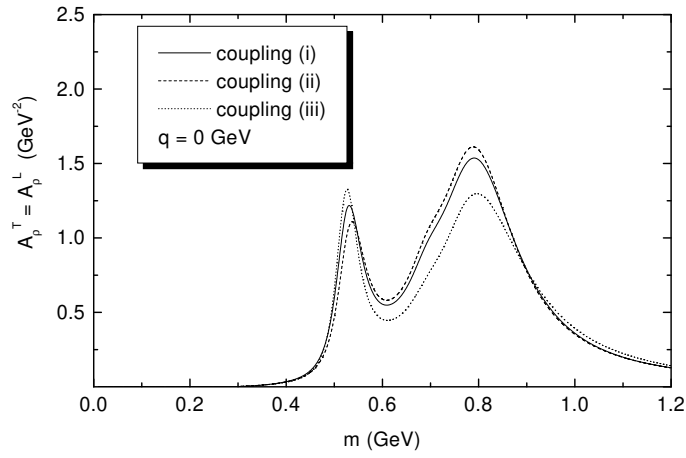


Figure 12: $A_\rho^T = A_\rho^L$ at $\mathbf{q} = \mathbf{0}$ GeV. The couplings employed for the calculations are explained in Sect. 6.

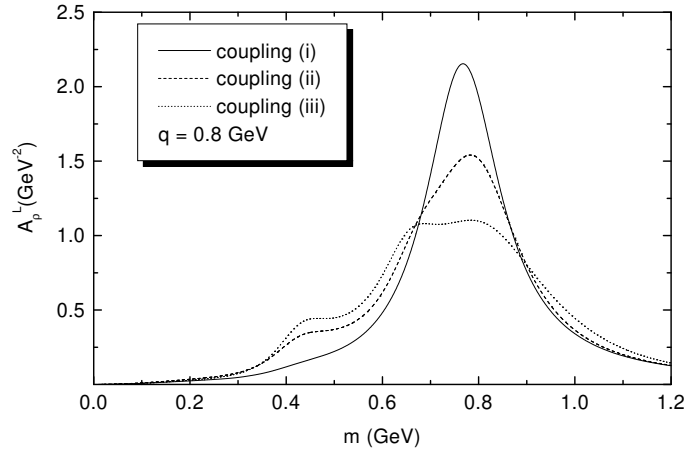
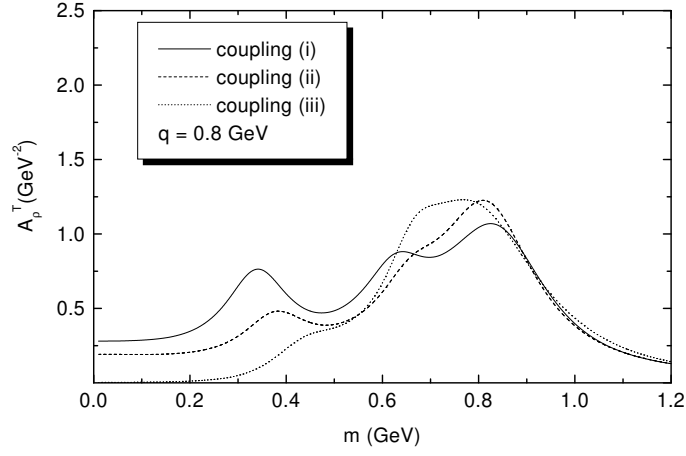


Figure 13: A_ρ^T (upper graph) and A_ρ^L (lower graph) at $\mathbf{q} = 0.8$ GeV. The couplings employed for the calculations are explained in Sect. 6.